ARTICLE

Detection of Bright Trion States Using the Fine Structure Emission of Single CdSe/ZnS Colloidal Quantum Dots

Mark J. Fernée,* Bradley N. Littleton,† and Halina Rubinsztein-Dunlop

Centre for Quantum Computer Technology, School of Physical Sciences, The University of Queensland, Queensland 4072, Australia. †Current address: Department of Physics, King's College London, the Strand, London WC2R 2LS, United Kingdom.

ABSTRACT We report direct observation of the lowest two states of the band-edge exciton fine structure in the photoluminescence from single CdSe/ZnS core/shell nanocrystals at cryogenic temperatures. The temperature dependence of this spectral fingerprint reveals exciton spin relaxation rates as low as 10 μs^{-1}. The fine structure is also dependent on the nanocrystal charge state facilitating the identification of a bright negatively charged trion state with a quantum yield comparable to that of neutral emission.

KEYWORDS: CdSe nanocrystals · quantum dots · trion · spin relaxation · exciton fine structure · single quantum dot spectroscopy

Highly symmetric spherical CdSe nanocrystals (NCs) possess a complex band-edge fine structure that is determined by the valence band spin−orbit interaction, hexagonal crystal structure, and the electron−hole symmetric exchange interaction. This splits an 8-fold degeneracy into five distinct levels, three of which contain allowed optical transitions and the other two containing "dark" forbidden transitions.[1,2] The lowest two states within the band-edge exciton fine structure correspond to an optically "bright" ($|F| = 1$) state lying above a "dark" ($|F| = 2$) state,[1,2] with a splitting determined by the electron−hole symmetric exchange interaction, which can range from approximately ~1 to 20 meV depending on the NC size. In distinct contrast with self-assembled quantum dots,[3−7] the dark $|F| = 2$ transition is not completely forbidden and can be observed in colloidal NCs, indicating the presence of some additional spin-mixing mechanism.[8−10] Even at the smallest splitting, efficient relaxation[1,8,9] often results in less than 1% of the population in the bright state at 5 K.[11] Nevertheless, time-resolved studies over a wide temperature range indicate that it is possible to thermally populate the upper bright state,[10,12] although this has not been confirmed spectroscopically. Thus, in principle, colloidal NCs can exhibit both dark and bright exciton emission as determined by the exciton fine structure.

Hitherto, spectroscopic measurements of single NCs at cryogenic temperatures have revealed only a single dark-state emission line.[11,13,14] The failure to spectroscopically detect the bright-state emission indicates that there is efficient relaxation from the upper bright state to the lower dark state, which requires a spin-flip of one of the charge carriers. Early measurements of the relaxation from the bright to the dark exciton state in bare CdSe cores found rates in the range of 0.1−0.01 ps^{-1},[1,8,9] which is between 2 and 3 orders of magnitude faster than the radiative relaxation rate of the bright state. A measurement of spin coherence in CdSe/ZnS core/shell NCs suggested a spin relaxation rate at least 10 times faster than the radiative relaxation rate of the bright state.[15] Nevertheless, we would expect to see emission from the upper bright state with increasing temperature due to a Boltzmann redistribution of population. For large NCs, with correspondingly narrow fine structure splittings, temperatures as low as 20 K should be sufficient for significant thermal population of the upper state. This provides a route to measuring the exciton spin relaxation rate from individual NCs.

The exciton fine structure is also dependent on the NC charge state, as there is no exchange interaction for a charged NC, and consequently no $|F| = 2$ dark state.[16,17] This should simplify the spectroscopic signature of a charged NC as there is only a single allowed optical transition near the band edge. In the case of spherical CdSe NCs with a heavy hole−light hole splitting of ~20 meV, it should only be possible to thermally populate the high energy excited states with temperatures approaching

*Address correspondence to fernee@physics.uq.edu.au.

Received for review August 15, 2009 and accepted October 9, 2009.

Published online October 16, 2009.
10.1021/nn9010158 CCC: $40.75

room temperature, and as such, the lowest charged state can be considered a single isolated state. Thus, the signature of a charged state should be a single spectral line at temperatures where one would expect to see fine structure emission. Such charged exciton states have received considerable attention for use in quantum technologies in applications such as spin storage, manipulation, and readout,[18] as well as single photon sources.[16] However, charged exciton states are usually weakly emitting due to strongly enhanced Auger scattering in NC quantum dots,[19−21] although recent reports suggest that Auger processes can be inhibited.[20,22−26]

In this report, we show that single CdSe/ZnS core/shell NCs can exhibit emission from both the $|F| = 1$ and $|F| = 2$ excitonic fine structure components. We reveal a clear size dependence of the fine structure splitting, which is directly attributable to hole confinement. The exciton spin relaxation rate is determined using the temperature dependence of the fine structure populations, and polarization-resolved spectroscopy is used to detect transitions between a neutral and an optically bright charged exciton state.

RESULTS AND DISCUSSION

Identification of Spectral Fine Structure. Ten percent of spectra observed from single CdSe/ZnS core/shell NCs at 5 K are doublets with a weak high energy peak, with the proportion of doublets increasing to ~50% between 10 and 20 K. The presence of discrete acoustic phonon side bands, previously identified as the symmetric $l = 0$ breathing mode,[27] indicates these NCs have a spherical shape (see Supporting Information, Figure S1). Correlated spectral diffusion is used to identify these two peaks as internal states of the NC.[27−29] In Figure 1a, we show the polarization-resolved detection of a spectral doublet. When the two orthogonal polarizations are added, we see that both spectral lines exhibit identical random frequency shifts (*i.e.*, spectral diffusion). These spectral shifts are related to fluctuations of the environmental charge configuration through the quantum confined Stark effect[14] according to $\partial\nu = 2\alpha_0(E_{int} + E_{env})\partial E_{env}$, where $\partial\nu$ is the spectral shift, α_0 is the polarizability of the excited state, E_{int} is the internal field, and E_{env} is the field due to the environmental charge configuration. Therefore, two spectral lines exhibiting perfectly correlated spectral fluctuations (as evidenced by identical line widths) must correspond to emitting states with identical polarizabilities and even more stringently identical excited-state dipoles. This would be true for two excitonic states (*e.g.*, two states within the $1S_{3/2}1S_e$ fine structure manifold) due to nearly identical charge confinement. Having identical polarizabilities also excludes emission from states with differing charge configurations, such as a trap or interface states. We also note that both peaks have LO phonon replicas, indicative of emission from intrinsic excitonic states (see Supporting Information, Figure S2).

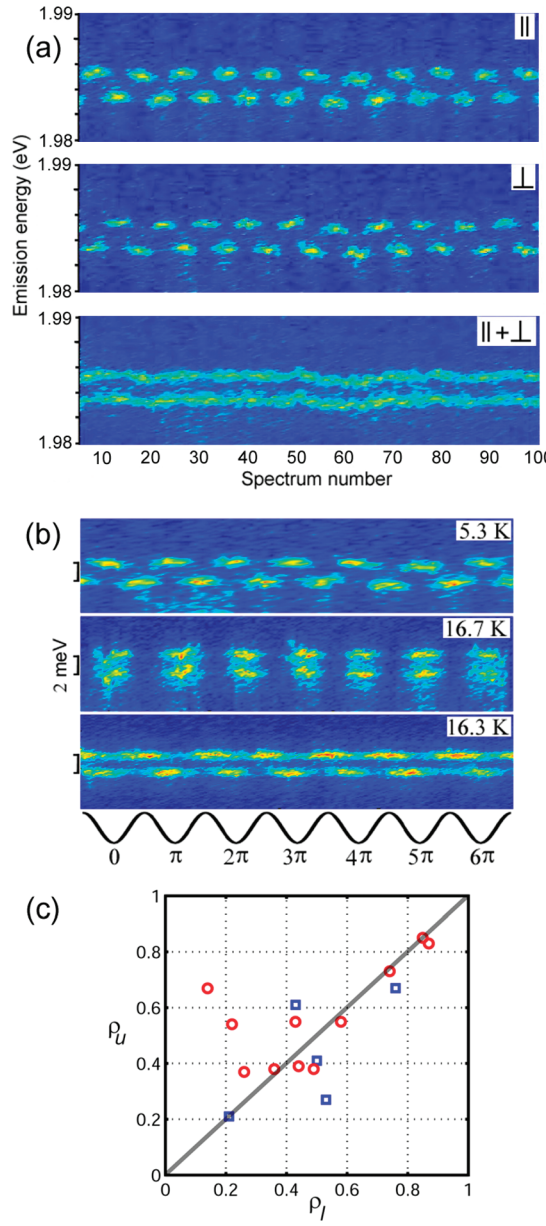

Figure 1. Polarization properties. (a) Polarization-resolved spectra acquired while continuously rotating the plane of polarization of the emission with a half-wave plate. An analyzer separates the two orthogonal linear polarizations, both of which are detected. The sum of the two channels gives the lower trace that exhibits highly correlated spectral diffusion of the two peaks. These data are obtained at 5.3 K and are used for Figure 3d. (b) Polarization-resolved spectra for three different single NCs with $R \sim 4$ nm cores and a pump irradiance of 40 W cm^{-2} integrating for 1 s. A vertical scale bar indicates a 2 meV energy separation. The horizontal scale represents the angle of a rotating half-wave plate. (c) Correlation in the degree of linear polarization $\rho = (P_\parallel - P_\perp)/(P_\parallel + P_\perp)$, between the upper (higher energy) and lower peaks of 16 different NCs ($R \sim 4$ nm core, circles; $R \sim 2.5$ nm core, squares).

Polarization-resolved measurements of spectral doublets indicate that the emission is from two distinct and different states. In Figure 1b, we show

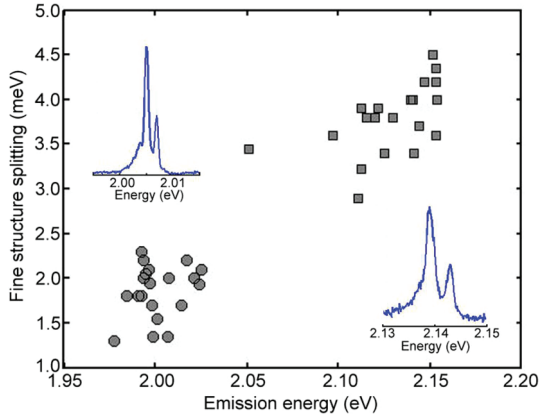

Figure 2. Plot of the doublet energy splitting as a function of the emission energy of the lowest energy spectral line. Twenty individual spectra from each of the two samples studied are presented ($R \sim 4$ nm core, circles; $R \sim 2.5$ nm core, squares). Example spectral doublets from each of the two samples are also included (inset).

polarization-resolved spectral doublets obtained from three individual NCs with $R \sim 4$ nm, while continuously rotating the polarization of the photoluminescence. The data illustrate that the polarization of each of the spectral lines is independent of the other, indicating that each of the two spectral peaks must result from states that are distinct from each other. In addition, the range of differing polarization projections between the two peaks excludes other possible splitting mechanisms such as splitting of the $|F| = 1$ bright state due to the anisotropic exchange interaction.[29] Another possibility, Zeeman splitting resulting in circularly polarized doublets, can be excluded as it should result in equivalent polarization projections, which is usually not the case with our data (as indicated by the first and third spectral series in Figure 1b).

In Figure 1c, we plot the degree of linear polarization of the doublet peaks obtained from 16 different NCs of both sizes. In most cases, the degree of linear polarization is found to be comparable (*i.e.*, correlated) over a wide range from $\rho = 0$ (unpolarized) to 1 (linearly polarized). This range of differing degrees of linear polarization is compatible with the previously observed emission from a degenerate dipole plane.[30] However, the generally differing polarization projections suggest the two states have *different* dipole planes. This is an unexpected result, although differing polarization projections have been predicted in large CdSe NCs, with the dark $|F| = 2$ state becoming polarized parallel to the crystal *c*-axis.[17]

The spectral doublets have a characteristic energy splitting that depends on the size of the core, as shown in Figure 2 (typical spectra obtained from the two NC sizes used in this study are shown in the inset). The correlation between the quantum-confinement-induced exciton emission energy and the doublet splitting energy indicates that the doublet splitting is dependent on the degree of quantum confinement. This is consistent with emission from excitonic fine structure states.[31] In fact, the measured doublet splitting energies are consistent with the splitting between the lowest bright $|F| = 1$ and dark $|F| = 2$ exciton lines obtained from CdSe NCs[1,2,32] and CdSe/ZnS NCs[12] of similar CdSe core size, indicating that the holes are predominantly confined to the cores in these NCs.

Determination of Exciton Spin Relaxation Rates. In Figure 3a,b, we show significant redistribution of the emission between the two spectral peaks as a function of temperature, consistent with a thermal Boltzmann redistribution. The ratio of peak heights as a function of temperature for three different NCs (including those represented in Figure 3a,b) is plotted in Figure 3c. The temperature dependence of the fine structure emission is well-described by a two-level rate equation model (Figure 3c, inset) solved in the steady state using detailed balance. The ratio of the two spectral features is then given by

$$\frac{S_U}{S_L} = \frac{n\gamma_{s\text{-}f}\Gamma_U + \lambda\Gamma_U\Gamma_L}{(n+1)\gamma_{s\text{-}f}\Gamma_L + (1-\lambda)\Gamma_U\Gamma_L} \qquad (1)$$

where, Γ_U, Γ_L, and γ_{s-f} are the upper level radiative decay, lower level radiative decay, and spin-flip rates, respectively; λ is the branching ratio of the hot carrier relaxation into the upper of the two states, $|U\rangle$ and $|L\rangle$, and $n = 1/[\exp(\Delta E_{UL}/k_BT) - 1]$ is the Bose−Einstein phonon occupation number for phonons of energy equivalent to the fine structure energy separation, ΔE_{UL}. We define the rates relative to the upper state radiative relaxation rate, Γ_U, which reduces eq 1 to a function of the normalized spin-flip rate, $\tilde{\gamma}_{s-f} \equiv \gamma_{s-f}/\Gamma_U$, the normalized lower state radiative relaxation rate $\tilde{\Gamma}_L \equiv \Gamma_L/\Gamma_U$, and temperature. This facilitates a two-parameter fit to the data. The fitting parameters for the two NCs indicated in Figure 3a,b indicate spin-flip rates comparable to the upper state radiative relaxation rate, Γ_U. In contrast, the third data set corresponds to a NC that exhibits rapid spin relaxation. The lower state radiative rates are also determined and found to be approximately 1 order of magnitude slower than the upper state radiative rate. These ratios are in excellent agreement with those obtained from the $|F| = 1$ bright and $|F| = 2$ dark exciton states using single NC lifetime measurements.[12]

The low-temperature region where the signal is approximately independent of temperature corresponds to the case, $n \approx 0$, and eq 1 can be reduced to $S_U/S_L = \lambda/(\tilde{\gamma}_{s-f} + (1-\lambda))$. This is independent of the lower level decay rate and can directly give the normalized spin-flip rate. The span of this low-temperature regime depends on the energy separation of the fine structure components, ΔE_{UL}. For the smaller level splitting around 1.9 meV, this region extends to temperatures around 4 K, while for the larger level separations (3.2 and 3.75 meV in Figure 3c), this region extends beyond 6 K. Spec-

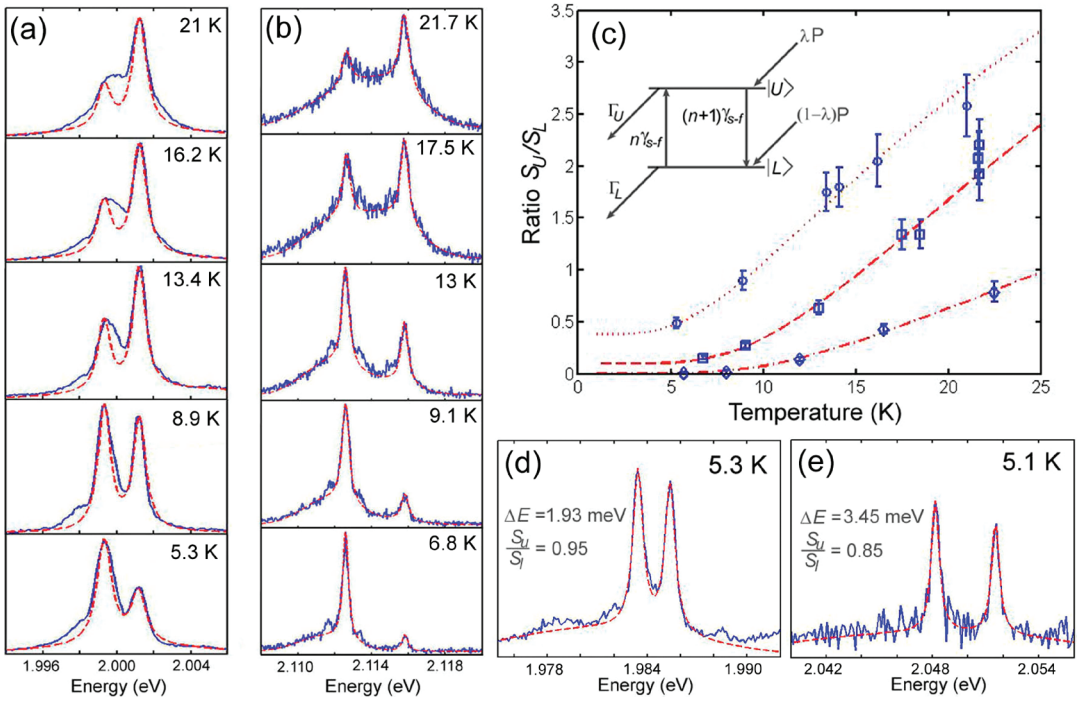

Figure 3. (a) Variation of a single NC spectrum with temperature obtained from a NC with $R \sim 4$ nm using a pump irradiance of 40 W cm^{-2}. (b) Variation of a single NC spectrum with temperature obtained from a NC with $R \sim 2.5$ nm using a pump irradiance of 27 W cm^{-2}. (c) Plot of the ratio S_U/S_L for the three NCs, including the NCs shown in panel a (circles) and panel b (squares), as a function of temperature. The dotted, dashed, and dot-dashed lines are fits to a solution to the steady-state rate equation described by the inset diagram, with parameters $\tilde{\gamma}_{s-f} = 0.8$, 4.5, 100, $\tilde{\Gamma}_L = 0.1$, 0.09, 0.18, and $\Delta E_{UL} = 1.9$, 3.2, 3.75 meV, respectively. (d) Doublet obtained from a single NC with $R \sim 4$ nm and a pump irradiance of 40 W cm^{-2}. (e) Doublet obtained from a single NC with $R \sim 2.5$ nm and a pump irradiance of 900 W cm^{-2}. The dashed red curves are fits to Lorentzian functions along with a Gaussian pedestal. The Lorentzian parameters are used to estimate the energy separation and ratio, S_U/S_L.

tra obtained from the larger NCs at temperatures near 5 K will fall just outside this asymptotic regime. However, spectra from the smaller NCs will lie in this temperature-independent regime, allowing straightforward measurement of the spin-flip rate.

In Figure 3d,e, we show two spectra taken near 5 K for both samples used in this study. Both show two strong emission lines separated by the appropriate energy spacing according to the trend in Figure 2. For the smaller NCs, a normalized spin-flip rate of $\tilde{\gamma}_{s-f} = 0.088$ is directly calculated from the ratio of emission strengths, $S_U/S_L = 0.85$. For the larger NCs, we estimate the spin-flip rate using eq 1 across a range of measured values for the dark exciton lifetime,[12] $\tilde{\Gamma}_L$, giving $\tilde{\gamma}_{s-f}$ in the range of 0.03 to 0.1. Curiously, these normalized rates are comparable to those found for *dark* exciton radiative decay. An average bright exciton radiative decay rate, $\Gamma_U = 0.1$ ns^{-1},[12] gives absolute spin-flip rates in the range of 1 to 10 μs^{-1}, which are more than 2 orders of magnitude slower than rates previously reported for CdSe NCs[1,8,9] and CdSe/ZnS core/shell NCs.[15]

Note: In determining the exciton spin relaxation rates, we have chosen a branching ratio of $\lambda = 0.5$ for the population rate of the bright and dark states. This is based on the data obtained from Labeau *et al.*,[12] where the absence of a fast decay exponent at high temperature indicates such a branching ratio. In our case, low-temperature spectra are indicative of the branching ratio. We have examined over 100 single NC spectra and find no evidence of spectral doublets at 5 K with a ratio, S_U/S_L, greater than 1, which would indicate a branching ratio with $\lambda > 0.5$ (although this may no longer be true with different CdSe/CdSZnS NCs; see Supporting Information, Figure. S3). A value of $\lambda > 0.5$ indicates residual spin coherence following hot carrier energy relaxation and in itself would be an indication of strongly inhibited spin-flips in the system.

Detection of Trion Emission. Transitions between neutral and charged exciton (trion) emission should provide a robust test of our state assignment, as the charged exciton has no dark state[16,17] and hence no band-edge fine structure. Charged excitons can occur when one of the charge carriers is trapped in a surface or lattice-defect state,[33] leaving a single unpaired charge carrier in the NC. Switching between doublet and singlet emission is indeed observed in some spectral series. In the polarization-resolved data, four clear cases of switching are found and all indicate that the *lower* energy state of the doublet switches *off* in the transition to the singlet state. This can be seen in Figure 4a,b, where the polarization projection of the higher energy state is maintained through the switching transition (indicated by vertical white lines), consistent with the lower dark state switching *off*. In Figure 4a, the intensity of the higher

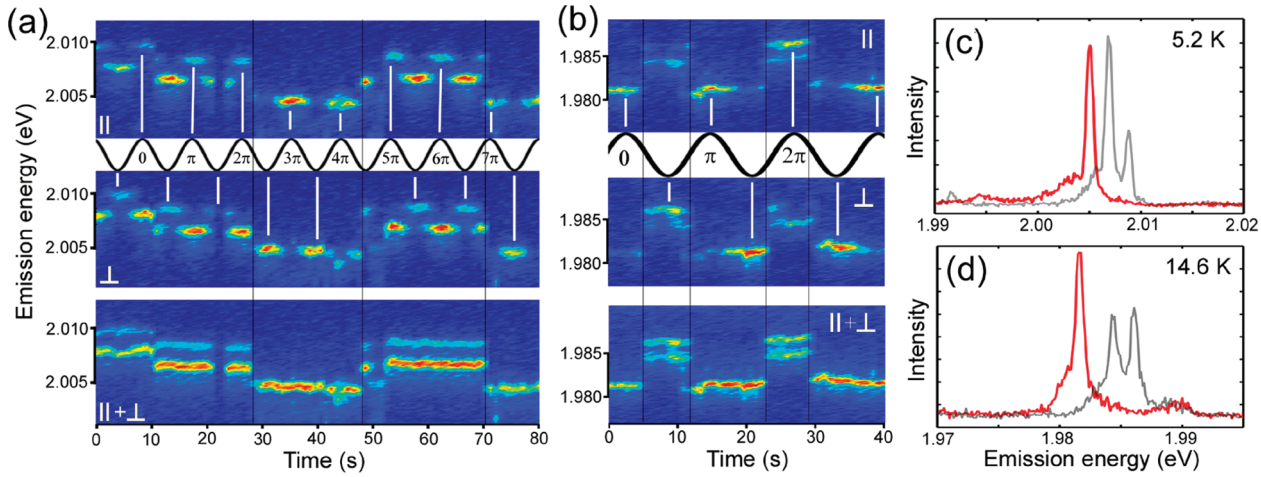

Figure 4. (a) Polarization-resolved spectra of a single NC with an $R \sim 4$ nm core obtained at 5.2 K with a pump irradiance of 40 W cm^{-2} integrating for 1.5 s. Two orthogonal polarization projections are shown along with the sum of the two projections. The phase angles correspond to the polarization projection obtained by rotating a half-wave plate. Black vertical lines indicate switching transitions, and white vertical lines follow polarization projection of the upper doublet state. (b) Polarization-resolved spectra of a single NC with an $R \sim 4$ nm core obtained at 14.6 K with a pump irradiance of 52 W cm^{-2} integrating for 1 s. (c) Comparison of the singlet and doublet spectra obtained in panel a. (d) Comparison of the singlet and doublet spectra obtained in panel b.

energy peak of the doublet is approximately one-third that of the lower energy peak, yet the polarization projection is maintained between the higher energy doublet peak and the singlet peak, and the total intensity is maintained through the transition (to within 10%; see Figure 4c). In Figure 4b, both peaks of the doublet have nearly equal intensity, and again, the total intensity is maintained through the transition (to within 5%; see Figure 4d). In all cases, the switching is accompanied by a small spectral red shift of up to 5 meV, identifying the negatively charged $X^{(-)}$ state[34,35] (note: in contrast, the positive trion is predicted and observed to have a considerably larger blue shift[34,21]). It is interesting to note that the $X^{(-)}$ trion is optically bright with no substantial loss of quantum yield, as indicated by Figure 4c,d, where we show that the integrated area of the singlet emission is within 90% of the total integrated area of the spectral doublets (note: this quantum yield estimation is approximately true for the weak excitation regime with pumping far above the band edge, where the density of states is approximately equal for both neutral and charged states).

The trion state is potentially of great technological value as it approximates a true two-level system with a well-defined spin,[16,18] although trion states in CdSe NCs have been implicated in photoluminescence blinking due to enhancement of the nonradiative Auger recombination in strongly quantum-confined NCs.[19] However, recent reports indicate that Auger scattering may be reduced in certain NC quantum dots.[20,22−26] In fact, it has been shown that careful NC core−shell engineering can completely inhibit Auger recombination to prevent blinking.[22,26] We observe blinking in the NCs studied here, so we cannot attribute such engineering to the observation of a bright trion state. Recent reports of a bright trion state[20,22−26,35] show a significant reduction in quantum yield. However, these studies were all conducted at room temperature, where energy conservation requirements of Auger recombination can be met *via* thermal broadening of the energy levels providing a quasi-continuum of final states. However, we report the first observation of the negative trion at cryogenic temperatures where there is significant line narrowing. Thus, we speculate that Auger recombination can be inhibited for the negative trion because of the comparatively low density of discrete electron states, which, when combined with narrow line widths, can inhibit Auger recombination assisted transitions to available single particle final states if there is an energy mismatch determined by energy conservation (*i.e.*, a mechanism analogous to the phonon bottleneck effect). In any case, the use of polarization-resolved fine structure switching allows robust identification of the trion state, indicating that efficient Auger recombination cannot be universal in these materials.

The fine structure emission we report here is unique to colloidal NCs, where $|F| = 2$ dark-state emission is commonly observed. In contrast, the dark state in self-assembled quantum dots is a nonemissive state, which only becomes emissive due to strong mixing with an applied magnetic field,[3,7] or otherwise, the presence must be inferred from photoluminescence dynamics.[4−6] Dark-state emission in colloidal NCs indicates the presence of some additional spin interaction peculiar to these materials, which has been the subject of some debate.[36−39] In any case, we have shown that the simultaneous detection of dark- *and* bright-state emission provides a spectral fingerprint that can be used to determine a number of useful properties. Thus, we report for the first time slow exciton spin relaxation rates comparable to theoretical expectation[40−43] and similar to rates determined in CdSe self-assembled quantum dots.[6] We are also able to show

that there can exist in colloidal CdSe NCs a bright negative trion, which has previously only been identified in self-assembled quantum dots.[3,6,44]

Finally, we note that not all spectra displayed doublets, even at elevated temperatures.[27] Given the observation of a bright negative trion, we can assume some proportion of the nanocrystals may be permanently charged, displaying only singlet (trion) emission. Another factor is that deviations from the spherical shape can significantly modify the spectrum.[28] In fact, from high-resolution electron microscope images, we found that our samples contain a significant proportion of nonspherical rod-shaped dots. Nevertheless, our data in Figure 2 are consistent with NCs with spherical cores, while the detection of discrete acoustic phonon side bands shows that the data we present originate from NCs with an overall spherical morphology. In other words, the detection of dots emitting spectral doublets provides a spectroscopic method for selecting spherical NCs from an ensemble.

CONCLUSIONS

We have observed and identified fine structure emission from the lowest $|F| = 1$ and $|F| = 2$ exciton states in single CdSe/ZnS NCs. The observation of spectral fine structure allows the determination of properties in single NCs that are otherwise hidden. Thus, we are able to determine the charge state of a single NC through the observation of transitions between singlet and doublet emission peaks. Bright emission from the $X^{(-)}$ trion was observed, with negligible reduction in quantum yield compared to neutral emission, contrary to expectation.

The temperature dependence of the fine structure was also used to probe the relaxation rate between the $|F| = 1$ and $|F| = 2$ exciton states, which requires a spin-flip. We found a wide variation in spin relaxation rates between different individual NCs covering over 3 orders of magnitude, from the well-established fast relaxation rates[1,15] to slow rates comparable to the dark exciton relaxation rate. Such a wide variation suggests that the exciton spin relaxation mechanism is not an intrinsic phenomenon in this material, as has been proposed for other quantum dots,[40−42] but rather an extrinsic phenomenon related to the surface and crystalline quality, which can vary between different NCs.

METHODS

Spectroscopic measurements were made on single CdSe/ZnS core/shell NCs sourced from a commercial supplier (Invitrogen ITK605 and ITK655 with core radii approximately 2.5 and 4 nm, respectively).[45] These materials were chosen due to their high room temperature quantum yield (~70 and ~80%, respectively) and their use in recent reports of efficient multiexciton generation.[46,47] The consequence of using commercial NCs is that the exact structure of the nanocrystal and surface ligand type is unknown. For example, the shell structure has been reported as either ZnS[31,45] or a compound CdZnS shell.[46,47] These discrepancies cannot be resolved as syntheses are likely to vary from batch to batch.

The sample was prepared by spin coating a dilute solution (10^{-11} M in decane) onto a crystal quartz substrate, which was mounted in a continuous flow liquid He cryostat (Oxford Instruments). Wide-field illumination with 532 nm laser light was used to excite the sample, enabling simultaneous detection of multiple NCs. Emission was collected by a 100× objective (Nikon, 0.7 NA), dispersed in a 300 mm imaging spectrometer, and detected with an electron multiplying CCD camera (Andor). Spectra were obtained using low pump irradiances (usually <100 W cm^{-2}) in order to prevent multiple photon absorption prior to radiative relaxation. For polarization-resolved measurements, a continuously rotating half-wave plate was placed in the detection path, and an analyzer consisting of a birefringent beam displacer was placed in front of the spectrometer entrance slit, dividing the image in two orthogonally polarized images, both of which were simultaneously detected on the CCD.

Acknowledgment. This work was supported by the Australian Research Council.

Supporting Information Available: Detection of discrete acoustic phonon side bands with spectral fine structure. Detection of LO phonon replicas of the fine structure states. Fine structure observed in CdSe NCs from a different source. This material is available free of charge *via* the Internet at http://pubs.acs.org.

REFERENCES AND NOTES

1. Nirmal, M.; *et al.* Observation of the Dark Exciton in CdSe Quantum Dots. *Phys. Rev. Lett.* **1995**, *75*, 3728−3731.
2. Efros, A.; *et al.* Band-Edge Exciton in Quantum Dots of Semiconductors with a Degenerate Valence Band: Dark and Bright Exciton States. *Phys. Rev. B* **1996**, *54*, 4843–4856.
3. Graham, T.; Curran, A.; Tang, X.; Morrod, J. K.; Prior, K. A.; Warburton, R. J. Direct and Exchange Coulomb Energies in CdSe/ZnSe Quantum Dots. *Phys. Status Solidi B* **2006**, *243*, 782–786.
4. Reischle, M.; Beirne, G. J.; Rossbach, R.; Jetter, M.; Michler, P. Influence of the Dark Exciton State on the Optical and Quantum Optical Properties of Single Quantum Dots. *Phys. Rev. Lett.* **2008**, *101*, 146402.
5. Kulakovskii, V. D.; Bacher, G.; Weigand, R.; Kummell, T.; Forchel, A.; Borovitskaya, E.; Leonardi, K.; Hommel, D. Fine Structure of Biexciton Emission in Symmetric and Asymmetric CdSe/ZnSe Single Quantum Dots. *Phys. Rev. Lett.* **1999**, *82*, 1780–1783.
6. Patton, B.; Langbein, W.; Woggon, U. Trion, Biexciton, and Exciton Dynamics in Single Self-Assembled CdSe Quantum Dots. *Phys. Rev. B* **2003**, *68*, 125316.
7. Puls, J.; Rabe, M.; Wunsche, H.-J.; Henneberger, F. Magneto-Optical Study of the Exciton Fine Structure in Self-Assembled CdSe Quantum Dots. *Phys. Rev. B* **1999**, *60*, R16303–R16306.
8. Nirmal, M.; Murray, C. B.; Bawendi, M. G. Fluorescence-Line Narrowing in CdSe Quantum Dots—Surface Localization of the Photogenerated Exciton. *Phys. Rev. B* **1994**, *50*, 2293–2300.
9. Bawendi, M. G.; Carroll, P. J.; Wilson, W. L.; Brus, L. E. Luminescence Properties of CdSe Quantum Crystallites—Resonance Between Interior and Surface Localized States. *J. Chem. Phys.* **1992**, *96*, 946–954.
10. Crooker, S. A.; Barrick, T.; Hollingsworth, J. A.; Klimov, V. I. Multiple Temperature Regimes of Radiative Decay in CdSe Nanocrystal Quantum Dots: Intrinsic Limits to the Dark-Exciton Lifetime. *Appl. Phys. Lett.* **2003**, *82*, 2793.

11. Empedocles, S. A.; Norris, D. J.; Bawendi, M. G. Photoluminescence Spectroscopy of Single CdSe Nanocrystallite Quantum Dots. *Phys. Rev. Lett.* **1996**, *77*, 3873–3876.
12. Labeau, O.; Tamarat, P.; Lounis, B. Temperature Dependence of the Luminescence Lifetime of Single CdSe/ZnS Quantum Dots. *Phys. Rev. Lett.* **2003**, *90*, 257404.
13. Empedocles, S. A.; Neuhauser, R.; Shimizu, K.; Bawendi, M. G. Photoluminescence from Single Semiconductor Nanocrystals. *Adv. Mater.* **1999**, *11*, 1243.
14. Empedocles, S. A.; Bawendi, M. G. Quantum-Confined Stark Effect in Single CdSe Nanocrystal Quantum Dots. *Science* **1997**, *278*, 2114–2117.
15. Gupta, J.; Awschalom, D.; Peng, X.; Alivisatos, A. Spin Coherence in Semiconductor Quantum Dots. *Phys. Rev. B* **1999**, *59*, R10421–R10424.
16. Strauf, S.; Stoltz, N. G.; Rakher, M. T.; Coldren, L. A.; Petroff, P. M.; Bouwmeester, D. High-Frequency Single-Photon Source with Polarization Control. *Nat. Photonics* **2007**, *1*, 704–708.
17. Califano, M.; Franceschetti, A.; Zunger, A. Lifetime and Polarization of the Radiative Decay of Excitons, Biexcitons and Trions in CdSe Nanocrystal Quantum Dots. *Phys. Rev. B* **2007**, *75*, 115401.
18. Kroutvar, M.; Ducommun, Y.; Heiss, D.; Bichler, M.; Schuh, D.; Abstreiter, G.; Finley, J. J. Optically Programmable Electron Spin Memory Using Semiconductor Quantum Dots. *Nature* **2004**, *432*, 81–84.
19. Klimov, V. I.; Mikhailovsky, A. A.; McBranch, D. W.; Leatherdale, C. A.; Bawendi, M. G. Quantization of Multiparticle Auger Rates in Semiconductor Quantum Dots. *Science* **2000**, *287*, 1011–1013.
20. Jha, P. P.; Guyot-Sionnest, P. Trion Decay in Colloidal Quantum Dots. *ACS Nano* **2009**, *3*, 1011–1015.
21. Shimizu, K. T.; Woo, W. K.; Fisher, B. R.; Eisler, H. J.; Bawendi, M. G. Surface-Enhanced Emission from Single Semiconductor Nanocrystals. *Phys. Rev. Lett.* **2002**, *89*, 117401.
22. Wang, X.; Ren, X. F.; Kahen, K.; Hahn, M. A.; Rajeswaran, M.; Maccagnano-Zacher, S.; Silcox, J.; Cragg, G. E.; Efros, A. L.; Krauss, T. D. Non-Blinking Semiconductor Nanocrystals. *Nature* **2009**, *459*, 686.
23. Osovsky, R.; Cheskis, D.; Kloper, V.; Sashchiuk, A.; Kroner, M.; Lifshitz, E. Continuous-Wave Pumping of Multiexciton Bands in the Photoluminescence Spectrum of a Single CdTe−CdSe Core−Shell Colloidal Quantum Dot. *Phys. Rev. Lett.* **2009**, *102*, 197401.
24. Spinicelli, P.; Buil, S.; Quélin, X.; Mahler, B.; Dubertret, B.; Hermier, J.-P. Bright and Grey States in CdSe−CdS Nanocrystals Exhibiting Strongly Reduced Blinking. *Phys. Rev. Lett.* **2009**, *102*, 136801.
25. Gómez, D. E.; van Embden, J.; Mulvaney, P.; Fernée, M. J.; Rubinsztein-Dunlop, H. Exciton−Trion Transitions in Single CdSe−CdS Core−Shell Nanocrystals. *ACS Nano* **2009**, *8*, 2281−2287.
26. Garcia-Santamaria, F.; Chen, Y.; Vela, J.; Schaller, R. D.; Hollingsworth J. A.; Klimov, V. I. Suppression of Auger Recombination in "Giant" Nanocrystals Boosts Optical Gain Performance. *Nano Lett.* DOI: 10.1021/nl901681d.
27. Fernée, M. J.; Littleton, B. N.; Cooper, S.; Rubinsztein-Dunlop, H.; Gómez, D. E.; Mulvaney, P. Acoustic Phonon Contributions to the Emission Spectrum of Single CdSe Nanocrystals. *J. Phys. Chem. C* **2008**, *112*, 1878–1884.
28. Le Thomas, N.; Herz, E.; Schöps, O.; Woggon, U.; Artemyev, M. V. Exciton Fine Structure in Single CdSe Nanorods. *Phys. Rev. Lett.* **2005**, *94*, 016803.
29. Furis, M.; Htoon, H.; Petruska, M. A.; Klimov, V. I.; Barrick, T.; Crooker, S. A. Bright-Exciton Fine Structure and Anisotropic Exchange in CdSe Nanocrystal Quantum Dots. *Phys. Rev. B* **2006**, *73*, 241313(R).
30. Empedocles, S. A.; Neuhauser, R.; Bawendi, M. G. Three-Dimensional Orientation Measurements of Symmetric Single Chromophores Using Polarization Microscopy. *Nature* **1999**, *399*, 126–130.
31. Biadala, L.; Louyer, Y.; Tamarat, Ph.; Lounis, B. L. Direct Observation of the Two Lowest Exciton Zero-Phonon Lines in Single CdSe/ZnS Nanocrystals. *Phys. Rev. Lett.* **2009**, *103*, 037404.
32. Woggon, U.; Gindele, F.; Wind, O.; Klingshirn, C. Exchange Interaction and Phonon Confinement in CdSe Quantum Dots. *Phys. Rev. B* **1996**, *54*, 1506–1509.
33. Cooney, R.; Sewall, S. L.; Dias, E. A.; Sagar, D. M.; Anderson, K. E. H.; Kambhampati, P. Unified Picture of Electron and Hole Relaxation Pathways in Semiconductor Quantum Dots. *Phys. Rev. B* **2007**, *75*, 245311.
34. Troparevsky, M. C.; Franceschetti, A. Radiative Recombination of Charged Excitons and Multiexcitons in CdSe Quantum Dots. *Appl. Phys. Lett.* **2005**, *87*, 263115.
35. Wang, C.; Wehrenberg, B. L.; Woo, C. Y.; Guyot-Sionnest, P. Light Emission and Amplification in Charged CdSe Quantum Dots. *J. Phys. Chem. B* **2004**, *108*, 9027–9031.
36. Califano, M.; Franceschetti, A.; Zunger, A. Temperature Dependence of Excitonic Radiative Decay in CdSe Quantum Dots: The Role of Surface Hole Traps. *Nano Lett.* **2005**, *5*, 2360–2364.
37. de Mello Donegá, C.; Bode, M.; Meijerink, A. Size- and Temperature-Dependence of Exciton Lifetimes in CdSe Quantum Dots. *Phys. Rev. B* **2006**, *74*, 085320.
38. Leung, K.; Pokrant, S.; Whaley, K. B. Exciton Fine Structure in CdSe Nanoclusters. *Phys. Rev. B* **1998**, *57*, 12291–12301.
39. Gupta, J. A.; Awschalom, D. D.; Efros, Al. L.; Rodina, A. V. Spin Dynamics in Semiconductor Nanocrystals. *Phys. Rev. B* **2002**, *66*, 125307.
40. Khaetskii, A.; Nazarov, Y. Spin Relaxation in Semiconductor Quantum Dots. *Phys. Rev. B* **2000**, *61*, 12639–12642.
41. Tsitsishvili, E.; Baltz, R. v.; Kalt, H. Exciton Spin Relaxation in Single Semiconductor Quantum Dots. *Phys. Rev. B* **2003**, *67*, 205330.
42. Roszak, K.; Axt, V. M.; Kuhn, T.; Machnikowski, P. Exciton Spin Decay in Quantum Dots to Bright and Dark States. *Phys. Rev. B* **2007**, *76*, 195324.
43. Paillard, M.; Marie, X.; Renucci, P.; Amand, T.; Jbeli, A.; Gerard, J. M. Spin Relaxation Quenching in Semiconductor Quantum Dots. *Phys. Rev. Lett.* **2001**, *86*, 1634–1637.
44. Akimov, I. A.; Hundt, A.; Flissikowski, T.; Kratzert, P.; Henneberger, F. Energy Spectrum of Negatively Charged Single Quantum Dot: Trion and Charged Biexciton States. *Physica E* **2003**, *17*, 31–34.
45. Liptay, T.; Marshall, L.; Rao, P.; Ram, R.; Bawendi, M. G. Anomalous Stokes Shift in CdSe Nanocrstals. *Phys. Rev. B* **2007**, *76*, 155314.
46. Fisher, B.; Caruge, J. M.; Zehnder, D.; Bawendi, M. Room-Temperature Ordered Photon Emission from Multiexciton States in Single CdSe Core−Shell Nanocrystals. *Phys. Rev. Lett.* **2005**, *94*, 087403.
47. Fisher, B.; Caruge, J. M.; Chan, Y.-T.; Halpert, J.; Bawendi, M. Multiexciton Fluorescence from Semiconductor Nanocrystals. *Chem. Phys.* **2005**, *318*, 71–81.